AIAA Guidance, Navigation, and Control Conference and Exhibit
16 - 19 August 2004, Providence, Rhode Island

AIAA 2004-5252

# AN ADAPTIVE VISION-BASED APPROACH TO DECENTRALIZED FORMATION CONTROL

Ramachandra Sattigeri [1] and Anthony J. Calise[2]
*School of Aerospace Engineering, Georgia Institute of Technology, Atlanta, GA 30332-0150*

Johnny H. Evers [3]
*Munitions Directorate, Air Force Research Laboratory, Eglin AFB, FL 32542-6810*

**In considering the problem of formation control in the deployment of intelligent munitions, it would be highly desirable, both from a mission and a cost perspective, to limit the information that is transmitted between vehicles in formation. In a previous paper, we proposed an adaptive output feedback approach to address this problem. Adaptive formation controllers were designed that allow each vehicle in formation to maintain separation and relative orientation with respect to neighboring vehicles, while avoiding obstacles. In this paper, we consider a modification to the adaptive control law that enables each vehicle in a leader-follower formation to track line-of-sight (LOS) range with respect to two or more neighboring vehicles with zero steady-state error. We also propose a coordination scheme in which each vehicle tracks LOS range to up to two nearest vehicles while simultaneously navigating towards a common set of waypoints. This coordination scheme does not require a unique leader for the formation, increasing robustness of the formation. As our results show, such *leaderless* formations can perform maneuvers like splitting to go around obstacles, rejoining after negotiating the obstacles, and changing into line-shaped formation in order to move through narrow corridors.**

## I. Introduction

As demonstrated in recent conflicts, unmanned aerial vehicles (UAVs) are becoming an important component of our military force structure. UAVs, operating in close proximity to enemy forces, provide real-time information difficult to obtain from other sources, without risk to human pilots. Among the weapons employed by these UAVs will be flocks of cooperative miniature or micro autonomous vehicles (MAVs) operating in close proximity to terrain or structures that will gather information on enemy movements and, under human supervision, seek out, identify, and attack targets of opportunity. In large groups of MAVs or small UAVs, even small percentage reductions in drag will offer significant increased payoffs in the ability to maintain persistent coverage of a large area. One concept, well known to bicyclists, race car drivers, and pilots and exploited by swimming and flying animals, is the benefit of operating in the wake of another vehicle (or organism). Therefore maintaining a formation while at the same time executing searches in a congested environment will be a primary requirement. Stealth like operations will also be important, implying the need to maintain autonomy and to minimize communication. Maintaining a formation is also important from this perspective so that passive (vision based) sensing can be used to ascertain the locations and behaviors of cooperating MAVs/UAVs.

Standard approaches for formation control include the leader-follower, behavior-based and the virtual structure approaches. In leader-follower based approach,[1,2] one vehicle is designated as a leader and the remaining vehicles as followers. The followers track the range from the leader and other followers to desired values. The leader sets a nominal trajectory for the formation to follow and may cooperate with the followers in regulating range. In the virtual structure approach, the entire formation is treated as a single entity.[3,4] Desired motion is assigned to this single entity, the virtual structure, which traces out trajectories for each member in the formation to track. In behavior-based approaches,[5,6] several desired behaviors are prescribed for each vehicle and the final control is

[1] Graduate Research Assistant, School of Aerospace Engineering, gte334x@prism.gatech.edu, AIAA Member
[2] Professor, School of Aerospace Engineering, anthony.calise@ae.gatech.edu, Fellow AIAA.
[3] Chief, Autonomous Control Team, evers@eglin.af.mil, Senior Member AIAA .

# Report Documentation Page

*Form Approved*
*OMB No. 0704-0188*



| 1. REPORT DATE | 2. REPORT TYPE | 3. DATES COVERED |
|---|---|---|
| **AUG 2004** | | **00-00-2004 to 00-00-2004** |

| 4. TITLE AND SUBTITLE | 5a. CONTRACT NUMBER |
|---|---|
| **An Adaptive Vision-Based Approach to Decentralized Formation Control** | 5b. GRANT NUMBER |
| | 5c. PROGRAM ELEMENT NUMBER |
| 6. AUTHOR(S) | 5d. PROJECT NUMBER |
| | 5e. TASK NUMBER |
| | 5f. WORK UNIT NUMBER |
| 7. PERFORMING ORGANIZATION NAME(S) AND ADDRESS(ES) **Georgia Institute of Technology,School of Aerospace Engineering,Atlanta,GA,30332-0150** | 8. PERFORMING ORGANIZATION REPORT NUMBER |
| 9. SPONSORING/MONITORING AGENCY NAME(S) AND ADDRESS(ES) | 10. SPONSOR/MONITOR'S ACRONYM(S) |
| | 11. SPONSOR/MONITOR'S REPORT NUMBER(S) |

12. DISTRIBUTION/AVAILABILITY STATEMENT
**Approved for public release; distribution unlimited**

13. SUPPLEMENTARY NOTES
**AIAA Guidance, Navigation, and Control Conference and Exhibit, 16-19 Aug 2004, Providence, RI. U.S. Government or Federal Rights License**

14. ABSTRACT

15. SUBJECT TERMS

| 16. SECURITY CLASSIFICATION OF: | | | 17. LIMITATION OF ABSTRACT | 18. NUMBER OF PAGES | 19a. NAME OF RESPONSIBLE PERSON |
|---|---|---|---|---|---|
| a. REPORT **unclassified** | b. ABSTRACT **unclassified** | c. THIS PAGE **unclassified** | **Same as Report (SAR)** | **24** | |

derived from a weighting of the relative importance of each behavior. Since in the leader-follower and virtual structure based approaches, coordination is with respect to a central agent, the formation controls lack robustness. Behavior-based approaches are decentralized and are significantly easier to implement. However, these are difficult to analyze mathematically and formation convergence to desired configurations is not guaranteed.

Although imperfectly understood, flocking behavior of birds, schooling behavior of fish, and even studies of swarming insects have provided inspiration for concepts of coordinated multi-vehicle operation.[7] Reynolds[8] introduced a model that suggests flocking is the combined result of three simple steering rules that each agent follows independently. In this model, each agent can access the whole scene's geometric description, but flocking requires that it react *only* to flock-mates within a certain small neighborhood. Reynolds rules were validated in a graph-theoretic and Lyapunov stability analysis framework.[9,10] Convergence properties on individual agent velocity vectors and relative distances were shown. Ref. 10 also provided a framework for addressing splitting, rejoining and squeezing maneuvers for flocks in the presence of multiple obstacles.

In our approach, we assume that the vehicles do not communicate velocity vector information. The lack of relative velocity vector information is treated as modeling uncertainty, whose effect on line-of-sight (LOS) range (output) regulation is to be canceled by the output of an online adaptive neural network (NN).[2] As a result, each vehicle can regulate both the range and relative orientation to a leader and/or neighboring vehicle without knowing the state and control policy of that vehicle. It is assumed that each vehicle can measure its own speed, heading, range and angle to other vehicles. The theory is based on an error observer approach to adaptive output feedback control of uncertain, MIMO systems.[11] The approach is adaptive to both parametric uncertainty and unmodeled dynamics. The method of Pseudo-Control Hedging (PCH) [12,13] is used to protect the adaptive process from actuator limits and actuator dynamics. It is also used to protect the adaptive process during periods when it is not in control of the vehicle.

In this paper, we modify the construction of the PCH signals so that each vehicle in a leader-follower formation tracks LOS ranges with respect to two or more neighboring vehicles with zero steady-state error. Because of the robustness issues associated with a leader-follower formation, we propose a coordination scheme that does not depend on a *unique* leader. In this scheme, which we call a *leaderless* formation scheme, each vehicle tracks LOS range to up to two nearest vehicles while simultaneously navigating towards a common set of waypoints. For a vehicle to be tracked, it must lie within a specified range from another vehicle. The *leaderless* nature of this scheme renders the formation robust to failures in one or more vehicles. Changes in the formation shape required while negotiating different obstacles are easier to implement using this approach. Since the number of vehicles that can be tracked using this approach is 0, 1, or 2, the control laws may be switching. Switching of the control laws can lead to the adaptive controller associated with tracking a particular neighboring vehicle to not be in control of the plant. In such cases, PCH is vital to the stability of the adaptation process.[18]

The organization of the paper is as follows. The next section summarizes the theory for the error observer approach and states the problem formulation for decentralized formation control. Next, we review the inverting control design for formation control. We also briefly discuss the static obstacle avoidance controller. Simulation results for a leader-follower team of 4 members regulating LOS range from each other are shown. Following this, the coordination scheme for *leaderless* formation flying is described. Simulation results with this scheme are shown for a team of 5 members. The results show splitting, rejoining and squeezing maneuvers in the presence of obstacles.

## II. ADAPTIVE OUTPUT FEEDBACK APPROACH

Consider the observable nonlinear system described by

$$\begin{aligned} \dot{x} &= f(x,u) \\ y &= g(x) \end{aligned} \tag{1}$$

where $x \in \Omega \subset \Re^n$ are the states of the system, $u, y \in \Re^m$ are the controls and regulated output variables respectively, and $f(\cdot,\cdot), g(\cdot)$ are uncertain functions. Moreover $n$ need not be known.

*1. Assumption*

The system in Eq. (1) satisfies the condition for output feedback linearizability with vector relative degree $[r_1, r_2, \ldots, r_m]^T$, $r = r_1 + r_2 + \ldots r_m \leq n$ .[14]

Then there exists a mapping that transforms the system into the so-called normal form:

$$\begin{aligned} \dot{\chi} &= f'(\xi, \chi) \\ \dot{\xi}_i^1 &= \xi_i^2 \\ &\vdots \\ \dot{\xi}_i^{r_i} &= h_i(\xi, \chi, u) \\ \xi_i^1 &= y_i, \; i = 1,2,\ldots,m, \end{aligned} \tag{2}$$

where $h_i(\xi, \chi, u) = h_i(x, u)$, where $\xi = \left[\xi_1^T \ldots \xi_m^T\right]^T$, $\xi_i = \left[\xi_i^1 \ldots \xi_i^{r_i}\right]^T$ and $\chi$ are the states associated with the internal dynamics. Note that $\xi_i^{j+1}$ is simply the $j^{th}$ time derivative of $y_i$ .

*2. Assumption*

The zero dynamics are asymptotically stable.

The objective is to design an output feedback control law that causes $y_i(t)$ to track a smooth bounded reference trajectory $y_{ci}(t)$ with bounded tracking error.

**A. Controller Design and Tracking Error Dynamics**

Feedback linearization is achieved by introducing the following inverse

$$u = \hat{h}^{-1}(y, \nu) \tag{3}$$

where

$$\nu = \hat{h}(y, u) \tag{4}$$

is the pseudo-control signal. The pseudo-control signal $\hat{h}(y,u) = \left[\hat{h}_1(y,u), \ldots, \hat{h}_m(y,u)\right]^T$ represents an invertible approximation to $h(x,u) = \left[h_1(x,u), \ldots, h_m(x,u)\right]^T$ in Eq. (2), which is limited to using only the available measurements and control signal. If outputs other than the regulated output are available for feedback, they may also be used in Eq. (3) to form the approximate inverse.

Thus the system dynamics, as far as the regulated output variable is concerned, is given by,

$$y^r = \nu + \Delta \tag{5}$$

where

$$\Delta(\xi,\chi,\nu) = h\left(\xi,\chi,\hat{h}^{-1}(y,\nu)\right) - \hat{h}\left(y,\hat{h}^{-1}(y,\nu)\right) \tag{6}$$

is the inversion error that results from the use of Eq. (3) in place of an exact state feedback inverse. The pseudo-control is chosen to have the form

$$\nu = y_c^r + \nu_{dc} - \nu_{ad} \tag{7}$$

where $y_c^r$ are generated by stable reference models that define the desired closed-loop behavior, $\nu_{dc}$ is the output of a dynamic compensator designed to stabilize the linearized error dynamics, and $\nu_{ad}$ is the adaptive component.

From Eq. (5) and Eq. (7), the error dynamics are given as,

$$\tilde{y}^r = y_c^r - y^r = -\nu_{dc} + \nu_{ad} - \Delta(x,\nu) \tag{8}$$

From Eq. (6) and Eq. (7) it is seen that $\Delta$ depends on $\nu_{ad}$ through $\nu$, and Eq. (8) shows that $\nu_{ad}$ has to be designed to cancel $\Delta$. Therefore the following assumption is introduced to guarantee existence and uniqueness of a solution for $\nu_{ad}$.

*3. Assumption*

The map $\nu_{ad} \mapsto \Delta$ is a contraction over the entire input domain of interest. It can be shown that this assumption leads to the following conditions[15]

$$\text{i) } \operatorname{sgn}\left(\frac{\partial h_i}{\partial u_i}\right) = \operatorname{sgn}\left(\frac{\partial \hat{h}_i}{\partial u_i}\right),\ i = 1,2,\ldots,m$$

$$\text{ii) } \left|\frac{\partial \hat{h}_i}{\partial u_i}\right| > \frac{1}{2}\left|\frac{\partial h_i}{\partial u_i}\right| > 0,\ i = 1,2,\ldots,m$$

The first condition requires that the sign of the control effectiveness is modeled correctly and the second places a lower bound on the estimate of the control effectiveness.

**B. Error Observer**

It can be shown that the error dynamics in Eq. (8) can be written as

$$\dot{E} = \overline{A}E + \overline{B}\left[\nu_{ad} - \Delta\right] \tag{9}$$

where the elements of *E* are made up of $\tilde{y}_i$ and its derivatives up to order $(r_i - 1)$ and the dynamic compensator states. An error observer is designed based on this equation,[11] which results in error estimates $\hat{E}$ that are used in the adaptive update law given below.

### C. Approximation of the Inversion Error

The inversion error $\Delta$ can be approximated to any desired degree of accuracy by using a Single Hidden Layer Neural Network (SHL NN) with sufficient number of hidden layer neurons, and having the following input vector,[16,17]

$$\bar{x}(t) = \left[1 \;\; \bar{v}_{\mathrm{d}}^{\mathrm{T}}(t) \;\; \bar{y}_d^T(t)\right]^T \tag{10}$$

where

$$\bar{v}_d^T(t) = \left[\nu(t), \nu(t-d), \ldots, \nu(t-(n_1-1)d)\right]^T,$$

$$\bar{y}_d^T(t) = \left[y(t), y(t-d), \ldots, y(t-(n_1-1)d)\right]^T$$

with $n_1 \geq n$. Since $n$ is unknown, a sufficient number of delayed signals are required. The input-output map of a SHL NN is given by

$$\nu_{ad} = W^T \sigma\left(V^T \bar{x}\right) \tag{11}$$

where $\sigma$ is the so-called squashing function. The NN is trained online with the adaptive law

$$\begin{aligned} \dot{W} &= -\Gamma_W \left[2\left(\sigma\left(V^T\bar{x}\right) - \sigma'\left(V^T\bar{x}\right)V^T\bar{x}\right)\hat{E}^T P\bar{B} + kW\right] \\ \dot{V} &= -\Gamma_V \left[2\bar{x}\hat{E}^T P\bar{B}W^T\sigma'\left(V^T\bar{x}\right) + kV\right] \end{aligned} \tag{12}$$

where $\sigma'(z) = \mathrm{diag}\left(\dfrac{\mathrm{d}\sigma_i}{\mathrm{d}z_i}\right)$, $P$ is the positive definite solution to the Lyapunov equation $\bar{A}^T P + P\bar{A} + Q = 0$, with $Q$>0, and $\Gamma_W$ and $\Gamma_V$ are the adaptation gains. It has been shown that the adaptive law in Eq. (12) guarantees (subject to upper and lower bounds on the adaptation gains) that all error signals and the NN weights are uniformly ultimately bounded.[11]

### D. Pseudo-Control Hedging (PCH)

PCH is introduced to protect the adaptive law from effects due to actuator limits (such as rate and position limits), unmodeled actuator dynamics and when the adaptive process is not in control of the plant.[12,13] The main idea behind PCH methodology is to modify the reference command, $y_c$, in order to prevent the adaptive element from adapting to these actuator characteristics. This is commonly done by generating the command using a reference model for the desired response. The reference model is 'hedged' by an amount equal to the difference between the commanded and an estimate for the achieved pseudo-control. To compute this difference, a measurement or estimate of the actuator position $\hat{u}$ is required. The pseudo-control hedge signal is given by,

$$\nu_{h_i} = \hat{h}_i\left(y, u_{cmd_i}\right) - \hat{h}_i\left(y, \hat{u}_i\right), \; i = 1,2,\ldots,m\,. \tag{13}$$

where $y_{cmd_i}$ is the external command signal, then the reference model update *with PCH* is set to

$$y_{c_i}^{r_i} = h_{rm_i}\left(y_{c_i}, \dot{y}_{c_i}, \ldots, y_{c_i}^{r_i-1}, y_{cmd_i}\right) - \nu_{h_i} \tag{14}$$

The instantaneous output of the reference model used to construct the pseudo-control signal remains unchanged and is given by

$$\nu_{rm_i} = h_{rm_i}\left(y_{c_i}, \dot{y}_{c_i}, \ldots, y_{c_i}^{r_i-1}, y_{cmd_i}\right) \tag{15}$$

The block diagram of the MRAC controller architecture with PCH and error observer is given below.

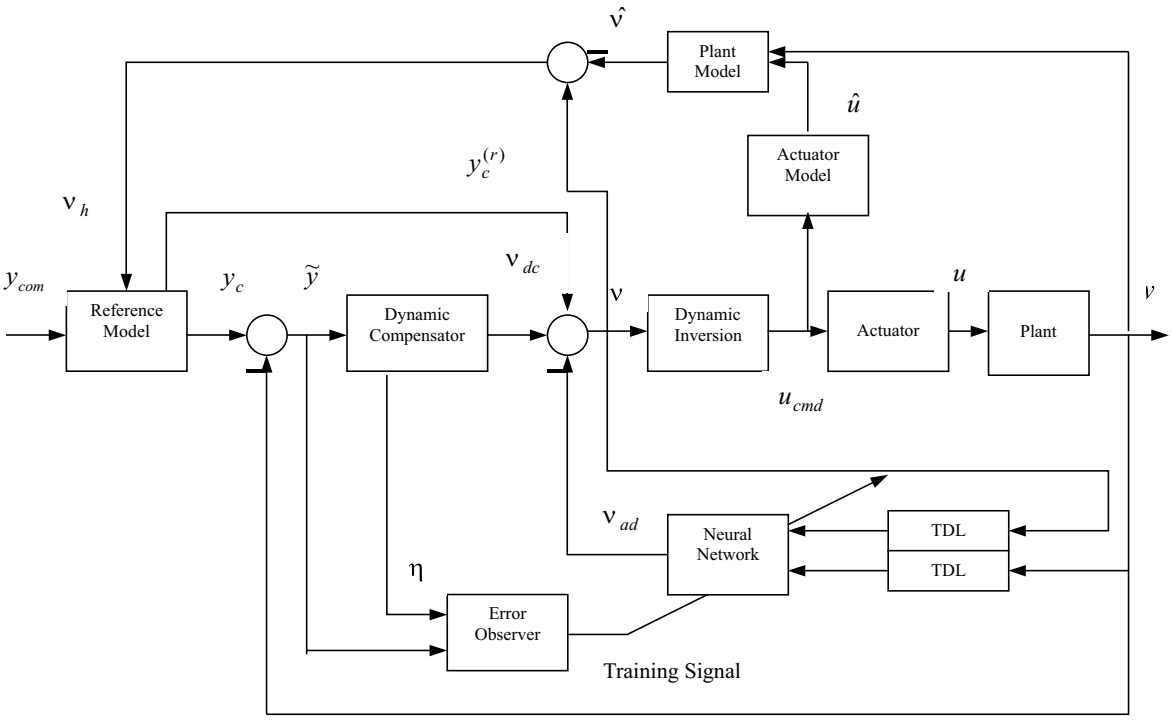


**Figure 1. MRAC Architecture with PCH**

## III. Formation Control Formulation

Consider a group of N vehicles whose individual dynamics are given by,

$$\dot{x}_i = f_i\left(x_i, u_i\right),\ i = 1,2,\ldots,N \tag{16}$$

where $x_i$ represents the states and $u_i$ the control vector of the $i^{th}$ vehicle. Assume that vehicles $i$ and $j$ cooperate by regulating a *joint* variable (e.g., LOS range)

$$z = g(x_i, x_j) \tag{17}$$

whose relative degree $(r)$ is known, so that,

$$z^{(r)} = g_r(x_i, x_{j,} u_i, u_j) \tag{18}$$

To arrive at a decentralized control solution, the following approximation is employed by the $i^{th}$ vehicle

$$z_i^{(r)} = \hat{g}_{ri}(z, x_i, u_i) = \nu_i \tag{19}$$

Equation (19) forms the basis for an inverting control design in which the inversion error is

$$\Delta_i = g_r(x_i, x_{j,} u_i, u_j) - \hat{g}_{ri}(z, x_i, u_i) \tag{20}$$

Vehicle $i^{'}s$ inverting solution is augmented with a NN that estimates and approximately cancels $\Delta_i$. The input vector to the NN for the $i^{th}$ vehicle is given by $\mu_i = [x_i, \bar{u}_{id}(t), \bar{z}_d(t)]^T$, where $\bar{u}_{id}(t), \bar{z}_d(t)$ are vectors of sufficiently large number of delayed values of $u_i(t), z(t)$ respectively.[16,17] So, the decentralized control solution of all cooperating aircraft is given by $u_i = \hat{g}_{ri}^{-1}(\nu_i, z, x_i)$, where $\nu_i$ is constructed as in Eq. (7).

## IV. APPLICATION TO FORMATION CONTROL

The formation of vehicles is constrained to lie in a two-dimensional plane. The vehicles are considered to be point-mass objects that can accelerate both along and perpendicular to the direction of motion. The non-dimensionalized equations of motion for the $i^{th}$ aircraft are given by [2]

$$\dot{x}_i = V_i \cos\psi_i \tag{21}$$

$$\dot{y}_i = V_i \sin\psi_i \tag{22}$$

$$\dot{\psi}_i = \frac{a_{i1}}{V_i} \tag{23}$$

$$\dot{V}_i = a_{i2} - k_{i1} V_i^2 - k_{i2}\left(\frac{a_{i1}^2 + 1}{V_i^2}\right) \tag{24}$$

where $(x_i, y_i)$ are the inertial position coordinates, $\psi_i, V_i$ are the heading and speed variables, $k_{i1}, k_{i2}$ are constants representing the effect of drag forces and $a_{i1}, a_{i2}$ are the controls representing non-dimensionalized acceleration. Bounds are placed on the controls to prevent slowing below the stall speed, and to prevent exceeding maximum bank angle limits and maximum and minimum longitudinal acceleration limits.[2] We model the actuator system as a saturation element with limits described above

$$u = \text{sat}(u_{cmd}) \tag{25}$$

Figure 2 shows the variables involved in describing the LOS kinematics. The LOS kinematics of the $i^{th}$ aircraft with respect to the $j^{th}$ aircraft is given by

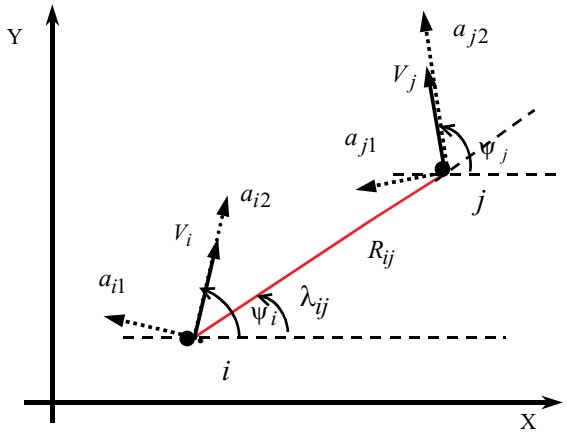


**Figure 2. LOS Kinematics**

$$\dot{R}_{ij} = V_j \cos(\psi_j - \lambda_{ij}) - V_i \cos(\psi_i - \lambda_{ij}) \tag{26}$$

$$\dot{\lambda}_{ij} = \frac{V_j \sin(\psi_j - \lambda_{ij}) - V_i \sin(\psi_i - \lambda_{ij})}{R_{ij}} \tag{27}$$

The information available to aircraft *i* include: $V_i, \psi_i$ (by use of an inertial measuring unit IMU), $R_{ij}, \lambda_{ij}$ (through vision-based sensors) and the control signals $a_{i1}, a_{i2}$.

### A. Adaptive Formation Control Design

We design an inverting controller augmented with a NN for aircraft *i* for regulating the LOS range $R_{ij}$ with respect to aircraft $j$. The controller architecture is as shown in Fig 1. The relative degree of $R_{ij}$ with respect to the speed and heading of aircraft *i* is 1. Hence the range command $R_{com}^{ij}$, for the separation between the aircraft $i$ and $j$, is filtered through a first order reference model. Figure 3 shows the hedged reference model. A rate limit is

introduced so that the reference model does not command large range rates when the range error is large. The parameter $p$ is the time constant and is a design parameter.

The dynamic compensator portion of the pseudo-control is a proportional error controller, $\nu_{dc(i,j)} = k_{p_i}\left(R_{c(i,j)} - R_{ij}\right)$. Referring to Eq. (7) the pseudo-control signal is

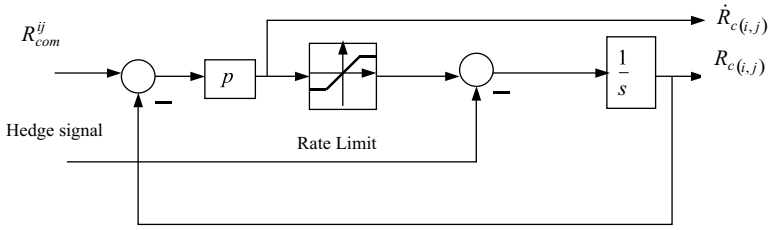


**Figure 3. Hedged Reference Model**

$$\nu_{(i,j)} = \dot{R}_{c(i,j)} + k_{p_i}\left(R_{c(i,j)} - R_{ij}\right) - \nu_{ad(i,j)} \tag{28}$$

The pseudo-control signal $\nu_{(i,j)}$ is the commanded LOS range-rate for aircraft $i$ with respect to aircraft $j$. The pseudo-control signal is inverted to give a commanded velocity vector $\vec{V}_{FC_i}$. In case aircraft $i$ is regulating LOS range with respect to multiple neighboring aircraft, say $m > 1$ in number, then the commanded velocity vector for aircraft $i$ is given by the vector sum of the pseudo-control signals oriented along $\lambda_{ij}$ [2]

$$\vec{V}_{FC_i} = -\sum_{j, j\neq i}^{m} \vec{\nu}_{(i,j)}, \tag{29}$$

$$\vec{\nu}_{(i,j)} = \nu_{(i,j)}\hat{\lambda}_{ij} = \nu_{(i,j)}\left(\cos\lambda_{ij}\hat{I} + \sin\lambda_{ij}\hat{J}\right) \tag{30}$$

where $\hat{\lambda}_{ij}$ is the unit vector along the LOS from aircraft $i$ to aircraft $j$, and $\hat{I}, \hat{J}$ are unit vectors aligned along the X and Y inertial axes respectively.

### B. Hedge Signals

Eq. (29)-(30) show that when commanding range with respect to $m > 1$ aircraft, we are actually trying to track $m$ pseudo-control signals with just one control variable, the velocity vector. This means each aircraft is an underactuated system when it commands range with respect to multiple aircraft. In this case, the method of calculating the hedge signal is special. We do a non-orthogonal projection of the actual velocity vector along each of the unit vector directions $\hat{\lambda}_{ij}$, $j = 1,\ldots m, j \neq i$. Each of these projections is treated as the achieved pseudo-control along the particular direction $\hat{\lambda}_{ij}$. The difference between the commanded pseudo-control and the achieved pseudo-control signal is the hedge signal. The actual mathematics for doing the above calculation is shown below.

$$\vec{V}_i = -\sum_{j,j\neq i}^{m} \alpha_{(i,j)}\hat{\lambda}_{ij} = -\overline{N}_{ij}[\vec{\alpha}_i] \tag{31}$$

where the $k^{th}$ column of $\overline{N}_{ij}$ is $\hat{\lambda}_{ik}$ and $[\vec{\alpha}_i]$ is the vector of elements $\alpha_{(i,j)}$, for all $j$, $j \neq i$. Note that $\alpha_{(i,j)}$ is the estimate of the achieved pseudo-control for aircraft $i$ along the direction $\hat{\lambda}_{ij}$.

Thus we can solve Eq. (31) to obtain

$$[\vec{\alpha}_i] = -\overline{N}_{ij}^{-1}\vec{V}_i \tag{32}$$

The corresponding expression for the PCH signal then becomes

$$\nu_{h_{(i,j)}} = \nu_{(i,j)} - \alpha_{(i,j)} \tag{33}$$

The hedge signals go to zero only when the LOS range equals the commanded range. This is an improvement over the preceding version of eq. (33) that resulted in steady-state errors whenever two or more aircraft were tracked.

The corresponding expression for inversion error $\Delta_{(i,j)}$ is given as

$$\Delta_{(i,j)} = \dot{R}_{ij} - \alpha_{(i,j)} \tag{34}$$

### C. Static Obstacle Avoidance

To illustrate the concept, it is assumed that the obstacles are contained within bounding spheres (circles in 2 dimensions), and that the centers $(X_o, Y_o)$ and radii $(r)$ of the obstacles are known. The goal of this strategy is to keep an imaginary line $L_o$ of length $D_o$, originating at the vehicle's current position and extending in the direction of the velocity vector, from intersecting with any obstacle boundary.[*] The length of this line is typically based upon the vehicle's speed and maneuverability. An obstacle further away than this length $D_o$ is not an immediate threat. The obstacle avoidance behavior considers each obstacle in turn and determines if they intersect with $L_o$. The obstacle which intersects $L_o$ nearest the aircraft is selected as the "most threatening" and corrective steering action is undertaken to avoid this obstacle. If no obstacle collision is imminent, no steering action is taken. Corrective steering action to avoid an obstacle involves a speed and heading change command. The heading change command $\Delta\psi_{OA_i}$ is towards the closest projected edge of the obstacle in the local velocity fixed frame as shown in Fig 4. The output of the static obstacle avoidance controller is the commanded velocity vector $\vec{V}_{OA}$. Please refer to Ref. [2] for details of constructing $\vec{V}_{OA}$.

[*] Craig Reynolds, "Not Bumping Into Things," *http://www.red3d.com/cwr/nobump/nobump.html*

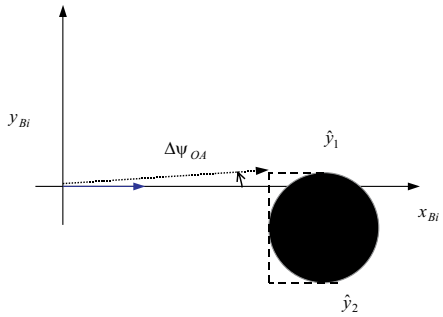


**Figure 4. Static Obstacle Avoidance**

### D. Velocity Command Blending

The composite velocity vector command is given by blending the outputs of the formation controller and the obstacle avoidance controller. The velocity command for a follower vehicle is

$$\vec{V}_{cmd_{foll}} = c_1 \vec{V}_{OA_{foll}} + (1 - c_1)\vec{V}_{FC_{foll}} \tag{35}$$

The weight $c_1$ is chosen such that obstacle avoidance has higher priority than formation control.[2] The velocity command for the leader vehicle is

$$\vec{V}_{cmd_{lead}} = c_1 \vec{V}_{OA_{lead}} + k(1 - c_1)\vec{V}_{FC_{lead}} + (1 - c_1 - k(1 - c_1))\vec{V}_L \tag{36}$$

where $\vec{V}_L$ is the leader component of velocity command for following a nominal trajectory. The factor $k$ is set equal to 0.2 implying that formation control is the lowest priority for the leader.

### E. Simulation Results

We consider a team of 4 aircraft flying in formation. Aircraft 1 is the team leader. It sets the trajectory for the formation by commanding a sequence of heading changes at specified time intervals $\psi_L(t)$ while commanding constant speed $V_L$. It is desired that the formation achieve the diamond-shape formation shown in figure 5 in the steady state. We specify a set of LOS range commands that are consistent with the desired formation shape. Cooperation between the aircraft is imposed by having all aircraft regulate LOS range from each other. The aircrafts are referenced by the indices 1, 2, 3, 4. The solid lines with arrow ends indicate desired steady-state velocity vectors for the aircrafts in formation.

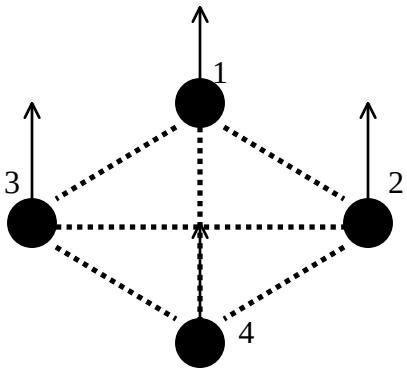


**Figure 5. Desired Formation Shape**

We present results for cases with adaptation (NN on) and without adaptation (NN off). Hedging is on (H on) only for NN on. Figures 6 and 7 show the trajectory plot of the formation with the NN off and NN on respectively. Aircraft 1 starts at (0,0), aircraft 2 at (6, -8), aircraft 3 at (-8, -6) and aircraft 4 at (0,-10). For the simulation, the following values of LOS ranges between pairs of aircraft were commanded:

$$R_{com}^{12} = R_{com}^{13} = R_{com}^{24} = R_{com}^{34} = 1.0$$
$$R_{com}^{14} = R_{com}^{23} = \sqrt{2} \tag{37}$$

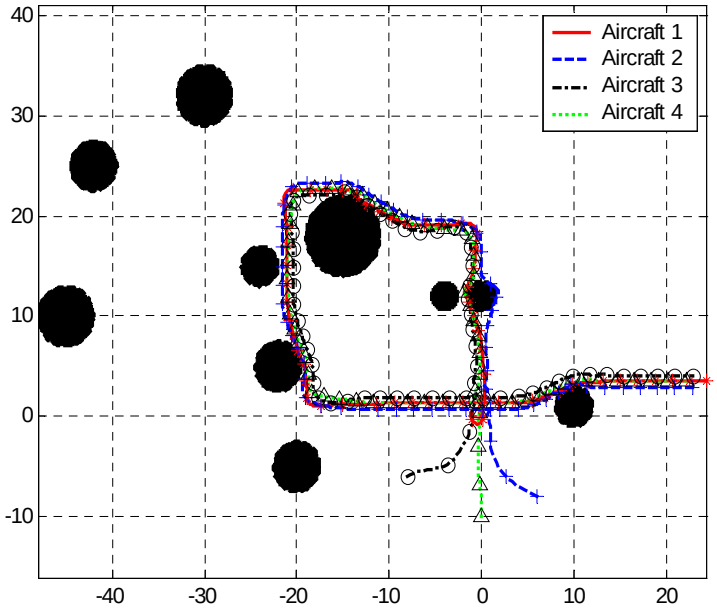


**Figure 6. Formation Trajectory (NN off)**

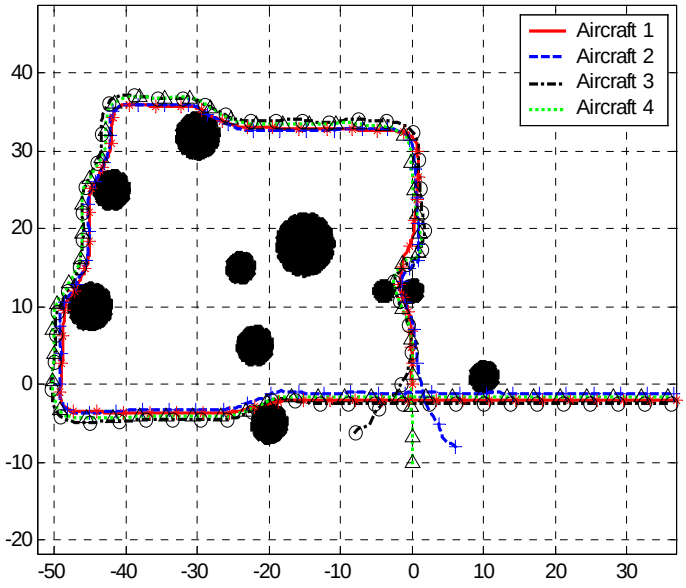


**Figure 7. Formation Trajectory (NN on)**

The desired formation shape is seen to be achieved when there are no obstacles in the path of the aircraft and when the leader vehicle is not commanding a heading change. The difference in the Figs 6 and 7 is the size of the box flown by the formation with NN on. This is because with NN on, the formation flies at the commanded speed of the leader $V_L$ in steady-state. With NN off, the leader slows down for the followers to catch up with it, and the formation flies at a lower speed in the steady state. We can thus infer that cooperation between the aircraft is enhanced with NN on. The speed histories for the formation with NN off and NN on are shown in Figs 8 and 9 respectively.

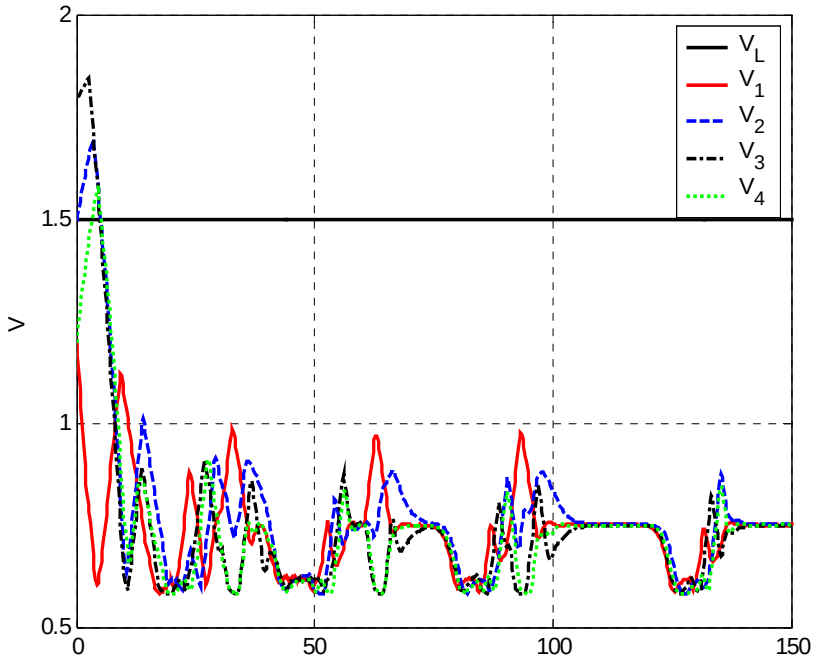


**Figure 8. Speed Histories (NN off)**

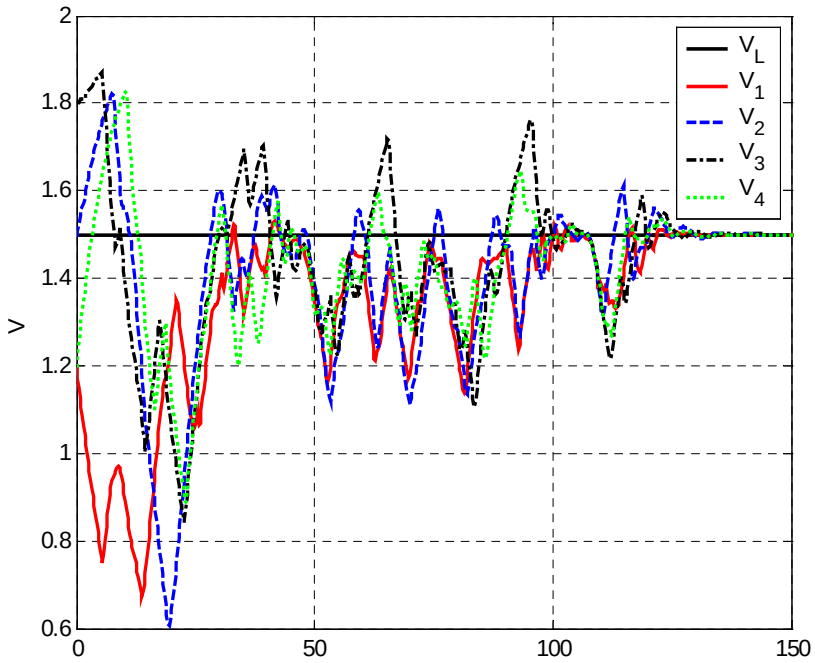


**Figure 9. Speed Histories (NN on)**

Figures 10 and 11 plot the error between the commanded range and the true range $\left(e_{ij} = R_{com}^{ij} - R_{ij}\right)$ between all pairs of aircraft. The plots show steady-state error in commanded range with NN off and zero steady-state error with NN on.


**Figure 12. Error in Commanded Range (NN off)**

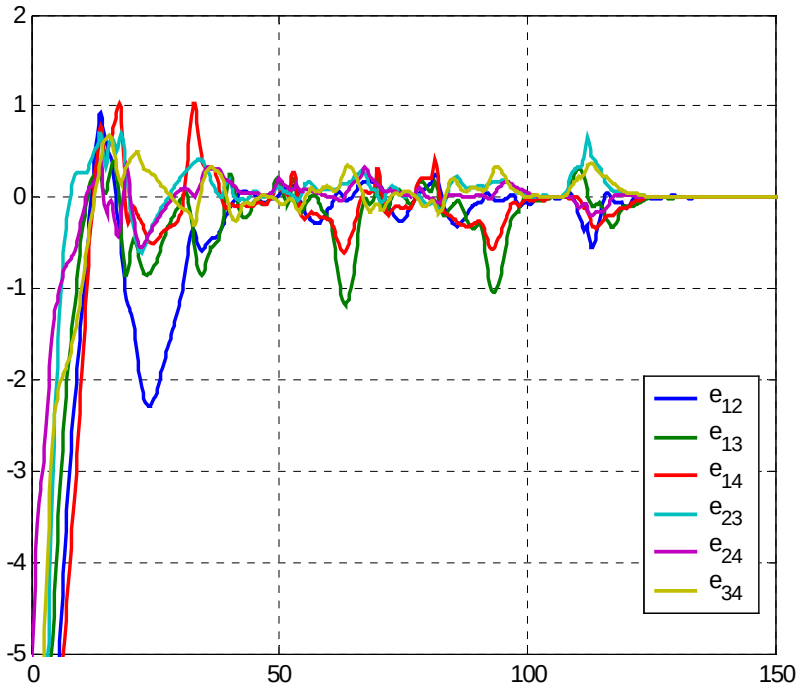


**Figure 11. Error in Commanded Range (NN on)**

## V. COORDINATION SCHEME FOR LEADERLESS FORMATION FLYING

The problem with a leader-follower formation control scheme is in the concept of a designated leader. Such a formation lacks robustness to a failure in the leader vehicle. Secondly, it is not practical to pre-specify LOS ranges between pairs of vehicles for large numbers of vehicles in formation. Possibilities of failure in one or more follower vehicles further complicate this problem. So, we propose a coordination scheme that does not depend on a unique leader, is robust to failures in one or more vehicles and allows easy scaling of the formation.

We remove the assumption of a designated leader for the formation. Each vehicle now commands a nominal velocity vector when not tracking any neighboring vehicle. The nominal velocity involves heading towards a set of waypoints at constant speed. The set of waypoints is common to all the vehicles. The nominal velocity vector $\vec{V}_{nom}$ is given as

$$\begin{aligned} V_{nom_i} &= V_L \\ \psi_{nom_i} &= a\tan 2\left(y_{WP} - y_i, x_{WP} - x_i\right) \end{aligned} \tag{38}$$

where $\left(x_{WP}, y_{WP}\right)$ represent inertial coordinates of the waypoints. Once the vehicle comes within a specified distance of one waypoint, it starts heading towards the next waypoint. The order in which the waypoints are tracked is the same for all vehicles.

Each vehicle tracks up to two nearest vehicles depending upon the range to the vehicle. The algorithm for choosing the number of vehicles to track is as follows.

Let $R_1(t)$ and $R_2(t)$ denote LOS ranges to two nearest vehicles. Let $R_{\max} > 0$ be a constant and $NV$ the number of vehicles tracked.

If $R_1(t) > R_{\max}$
    $NV = 0$
Elseif $R_2(t) \le R_{\max}$
    $NV = 2$
Else
    $NV = 1$
End

**Figure 12. Logic for Choosing Number of Vehicles to Track**

The formation control objective is to regulate range from $NV$ number of nearest vehicles to $R_{com}$. The value for $R_{com}$ is such that $0 < R_{com} < R_{\max}$ and is a constant for all the vehicles in the formation.

When the number of nearest neighbors $NV$ changes, the control law switches. Switching of the control laws also takes place when a nearest neighbor is replaced.

We design adaptive formation controllers to regulate LOS range from every vehicle in the formation, but tracking takes place only with $NV$ number of neighbors. The implication is that not all adaptive controllers are in control of the plant, and switches can take place between the adaptive controllers that are in control of the plant. PCH allows adaptation to continue safely when not in control of the plant.[18]

Since the number of vehicles tracked may change in time, the commanded velocity vector also changes. Let $\lambda_1(t)$ and $\lambda_2(t)$ denote LOS angles with respect to the two closest vehicles, $\hat{\lambda}_1(t)$ and $\hat{\lambda}_2(t)$ the associated LOS unit vectors, and $\vec{V}_{FC_1}$ and $\vec{V}_{FC_2}$ the commanded velocity vectors for regulating range from the two closest vehicles. Then, the velocity vector command is given as

$$\text{If} \quad NV = 1$$
$$\vec{V}_{cmd} = c_1\vec{V}_{OA} + (1-c_1)\left(\vec{V}_{nom} - k(1-c_1)\left\langle \vec{V}_{nom} \bullet \hat{\lambda}_1 \right\rangle \hat{\lambda}_1\right) + k(1-c_1)\vec{V}_{FC_1} \tag{39}$$

$$\text{If} \quad NV = 2$$
$$\vec{V}_{cmd} = c_1\vec{V}_{OA} + (1-c_1)\left(\vec{V}_{nom} - k(1-c_1)\left[\left\langle \vec{V}_{nom} \bullet \hat{\lambda}_1 \right\rangle \hat{\lambda}_1 + \left\langle \vec{V}_{nom} \bullet \hat{\lambda}_2 \right\rangle \hat{\lambda}_2\right]\right) + k(1-c_1)\left[\vec{V}_{FC_1} + \vec{V}_{FC_2}\right] \tag{40}$$

$$\text{If} \quad NV = 0$$
$$\vec{V}_{cmd} = c_1\vec{V}_{OA} + (1-c_1)\vec{V}_{nom} \tag{41}$$

where $\langle \bullet \rangle$ is the dot product operator, and $k > 0$ is a tuning parameter that indicates the relative priority for formation control with respect to nominal velocity vector tracking.

Eq. (39) and (40) are constructed with the objective that the velocity vectors should converge to $\vec{V}_{nom}$ when the commanded range errors are zero, $\vec{V}_{nom}$ is the same for all vehicles, and when there are no obstacles to avoid. This can be understood by noting that $\left\langle \vec{V}_{nom} \bullet \hat{\lambda}_1 \right\rangle \hat{\lambda}_1$ $\left[\left\langle \vec{V}_{nom} \bullet \hat{\lambda}_2 \right\rangle \hat{\lambda}_2\right]$ is the projection of $\vec{V}_{nom}$ along the unit vector direction $\hat{\lambda}_1$ $(\hat{\lambda}_2)$, and $\vec{V}_{FC_1}$ $(\vec{V}_{FC_2})$ is an estimate of the velocity of the closest (second closest) neighbor along $\hat{\lambda}_1$ $(\hat{\lambda}_2)$ when the commanded range errors are zero. So, the desired equilibrium configuration for the formation is not reached unless $\left\langle \vec{V}_{nom} \bullet \hat{\lambda}_1 \right\rangle \hat{\lambda}_1$ $\left[\left\langle \vec{V}_{nom} \bullet \hat{\lambda}_2 \right\rangle \hat{\lambda}_2\right]$ equals $\vec{V}_{FC_1}$ $(\vec{V}_{FC_2}) \Rightarrow \vec{V}_{cmd} = \vec{V}_{nom}$.

### F. Simulation Results

The first set of results with the leaderless formation control scheme is shown for a group of 4 aircraft with identical nominal velocity vectors $\vec{V}_{nom}$.

The nominal velocity vector is a sinusoidal heading profile at constant speed

$$\begin{aligned} V_{nom} &= 1.5 \\ \psi_{nom} &= \sin\left(t/5\right) \end{aligned} \tag{39}$$

The value of $R_{com}$ chosen is $0.5$. The initial positions of the aircraft were chosen such that each aircraft was tracking 2 neighboring aircraft. Figure 13 shows the trajectory plot for the formation. Note that the dimensions along the x-axis have been scaled up in the plot below.

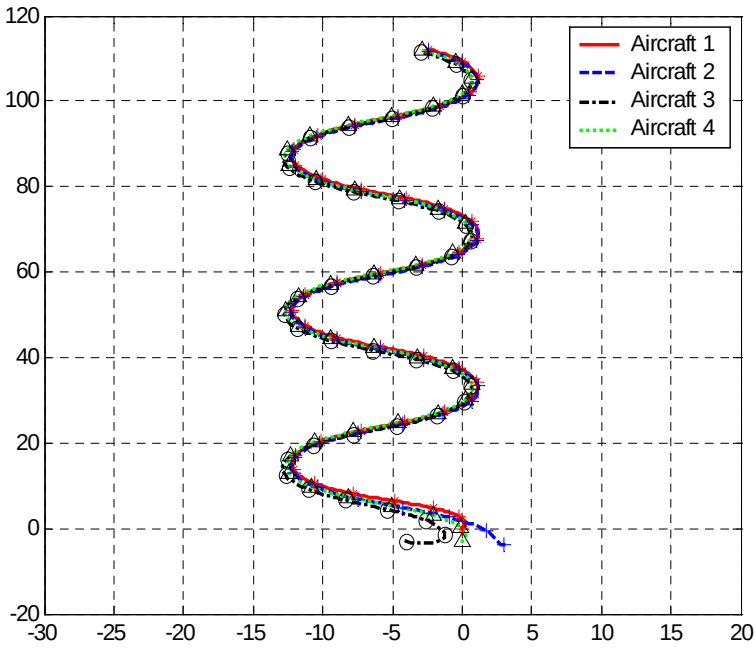


**Figure 13. Leaderless Formation Trajectory for Identical Nominal Velocity**

Figure 13 shows the LOS range histories for all aircraft in formation. The plot shows convergence to the commanded range $R_{com}$ of the LOS ranges from the 2 closest neighbors for all aircraft. The plot also shows that aircraft 1 and 3 are separated by a range larger than $R_{com}$ in steady-state, and that aircraft 2 and 4 seem to be at the commanded range from all aircraft. This suggests that the formation has split into 2 groups with aircrafts 2 and 4 common to both groups. The splitting of the formation is a common result with the leaderless formation control scheme.

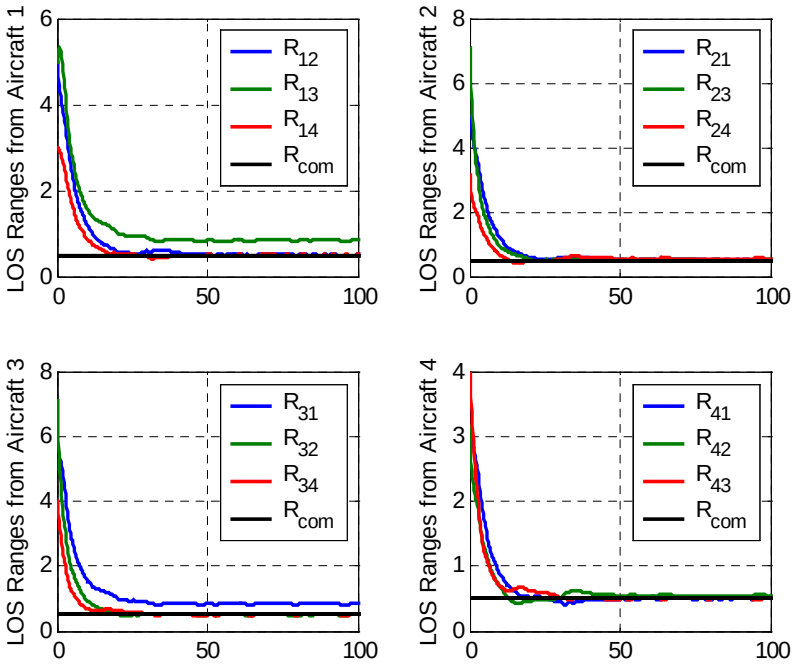


**Figure 13. LOS Range Histories for Leaderless Formation**

Figure 14 shows the plot of some of the inversion errors $\Delta_{ij}$ plotted against the corresponding NN outputs $\nu_{ad_{(i,j)}}$. The plot shows very good tracking of the $\Delta_{ij}$. Note in particular the first subplot. The signal $\nu_{ad(1,3)}$ is the NN output of aircraft 1 designed to track aircraft 3. From figure 13, we know that aircraft 1 does not track aircraft 3 because aircraft 2 and 4 are its closest neighbors. This shows that adaptation continues despite the adaptive control not being in control of the plant.

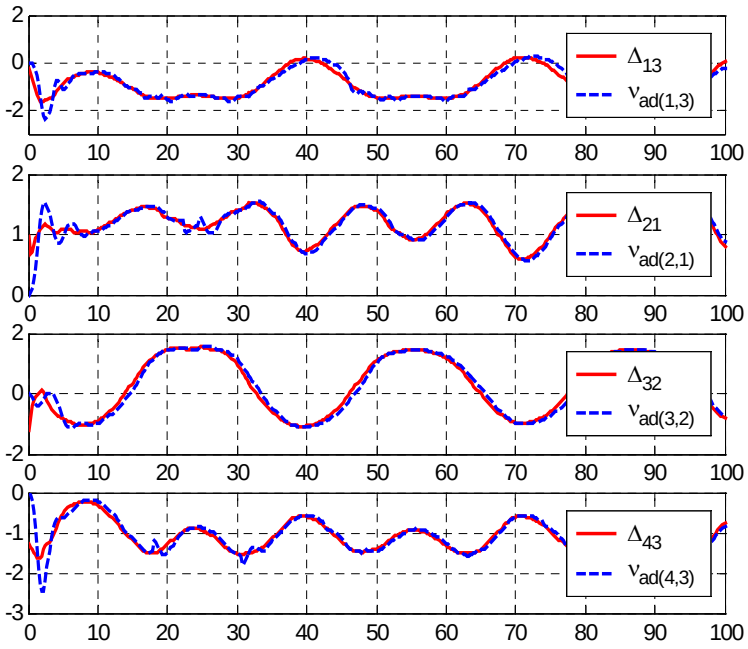


**Figure 14. Inversion Error and NN outputs**

Next we consider a group of 5 aircraft tracking a sequence of waypoints in the counter-clockwise direction. Figure 15 shows the trajectory of the formation. Waypoints are marked in the plot by red crosses. The plot shows that the formation is achieved and maintained at places where there are no obstacles. The formation is also seen to split to go around an obstacle and later rejoin.

Figure 16 shows the LOS ranges between all pairs of aircraft in the formation. It can again be concluded that the formation has split into groups by noting that only some of the LOS ranges have converged to the commanded value $R_{com}$.

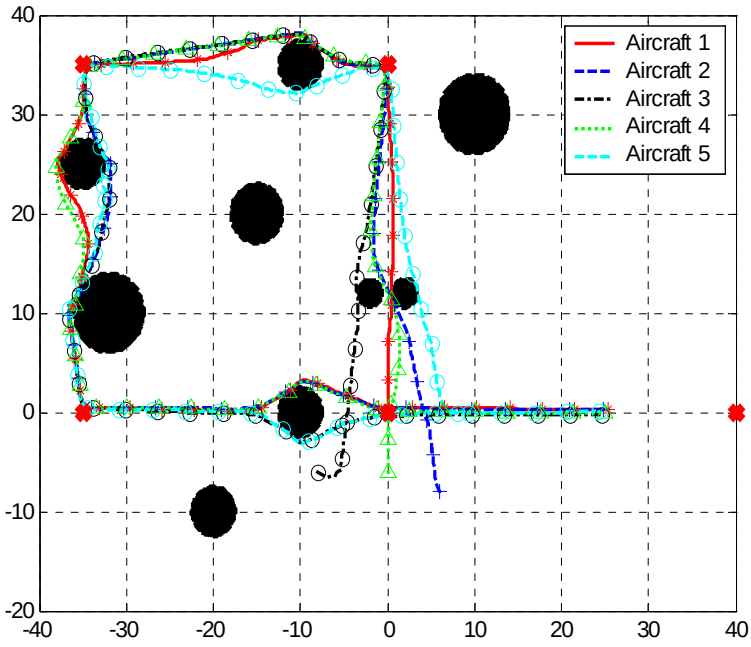


**Figure 15. Leaderless Formation Trajectory with Waypoint Tracking**

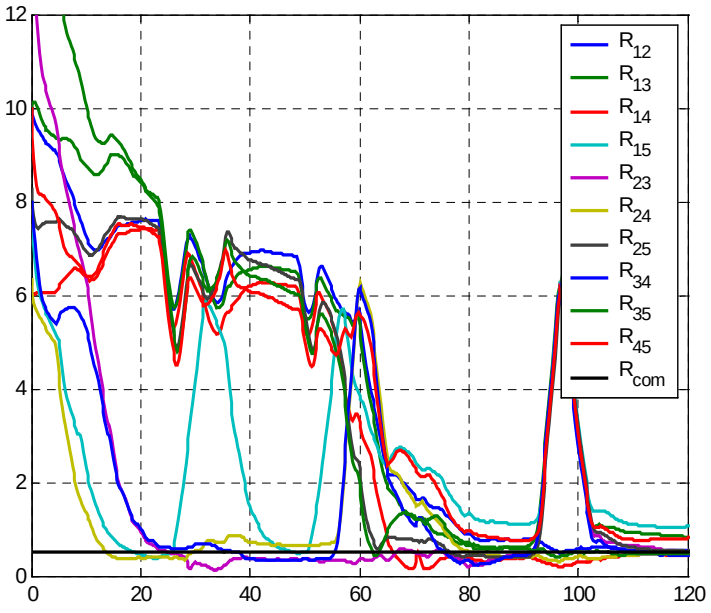


**Figure 16. LOS Range Histories for Leaderless Formations with Waypoint Tracking**

Figure 17 shows the number of vehicles being tracked by every vehicle during the maneuver. The number of neighboring vehicles tracked is seen to change in time.

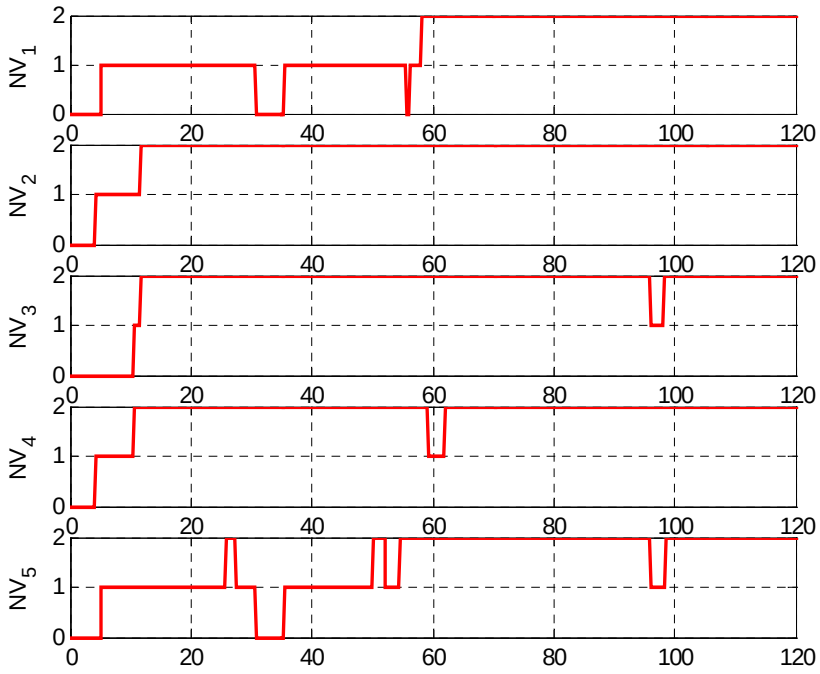


**Figure 17. Number of Neighbor Vehicles (*NV*) Tracked**

Figure 18 shows a maneuver in which the formation changes from a wide formation to a line-shaped formation. Line-shaped formations are desirable when the formation is required to squeeze through narrow corridors. The line-shaped formation is achieved when each vehicle tracks the nearest vehicle that lies in a conical region in front of it. When there are no vehicles in this conical region, each vehicle has nominal motion directed towards a waypoint. This waypoint is common to all vehicles and can be considered to be a point at the entrance of the narrow corridor.

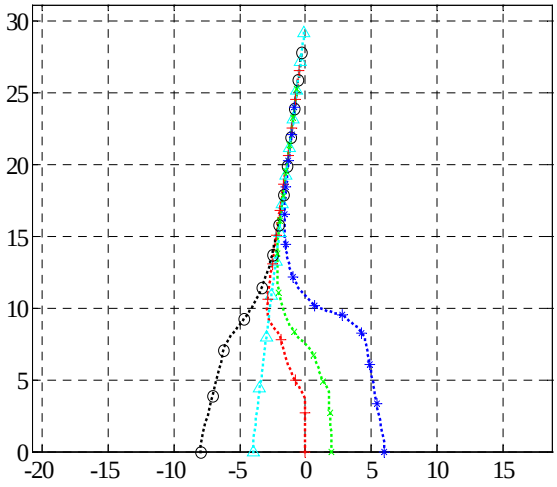


**Figure 18. Transition to Line-Shaped Formation**

## VI. CONCLUSIONS

We have formulated a decentralized adaptive guidance strategy that enables safe and coordinated motion of a group of unmanned vehicles in an environment with obstacles. We have shown that adaptation benefits by enhancing the cooperation between the vehicles in formation.

We have implemented two coordination schemes for formation control: leader-follower formation scheme and leaderless formation scheme. In the adaptive leader-follower formation scheme, we have modified the PCH signal construction to enable the tracking of two or more LOS range variables with zero steady state error. This is an improvement over our preceding result. The leaderless formation control scheme is proposed as a way of dealing with the robustness issues of the leader-follower formation control scheme. The decentralized formations that result from the application of this scheme can perform maneuvers like splitting / rejoining around obstacles and changing into line-shaped formation in order to move through narrow corridors.

## ACKNOWLEDGMENTS

This research has been sponsored under AFOSR contract F4960-01-1-0024 and under NRTC contract NCC 2-945.

## REFERENCES

[1]Das, A.V., Fierro, R., Kumar, V., Ostrowski, J.P., Spletzer J., Taylor, C.J., "A Vision-based Formation Control Framework," *IEEE Transactions on Robotics and Automation*, Vol. 18, No. 5, October 2002, pp. 813-825.

[2]Sattigeri, R., Calise, A.J. and Evers, J., "An Adaptive approach to Vision-based Formation Control," *AIAA-2003-5727 Guidance, Navigation and Control Conference*, Austin, TX, August 2003.

[3]Beard, R.W., Lawton J., and Hadeagh, F.Y., "A Feedback Architecture for Formation Control," *Proc. of the American Control Conference*, Vol. 6, June 2000, pp. 4087-4091.

[4]Leonard, N.E., and Fiorelli, E., "Virtual Leaders, artificial potentials and coordinated control of groups," *IEEE Conf. Decision and Control,* Fl, Dec 2001, pp. 2968 - 2973.

[5]Balch, T., and Arkin, R.C., "Behavior-based Formation Control for multi-robot teams," *IEEE Trans. Robot. Automat.,* Vol. 14, Nov 1998, pp. 926-934.

[6]Mataric, M., *Interaction and Intelligent Behavior*. PhD thesis, MIT, EECS, 1994.

[7]Bonabeau, E., Dorigo, M., Theraulaz, G., *Swarm intelligence: from natural to artificial systems,* Oxford University Press, 1999.

[8]Reynolds, C.W., "Flocks, Herds and Schools: a Distributed Behavioral Model," Computer Graphics, 21(4): 71-87,1987.

[9]Tanner, H.G., Jadbabaie, A., and Pappas, G.J., "Stable Flocking of Mobile Agents, Part I: Fixed Topology," *IEEE Conf. Decision and Control,* Hawaii, December 2003, pp. 2010-2015.

[10]Olfati, S., and Murray, R.M., "Flocking with Obstacle Avoidance: Cooperation with Limited Communication in Mobile Networks," *Proceedings of the IEEE Conference on Decision and Control,* Hawaii, December 2003.

[11]Hovakimyan, N., and Calise, A.J., "Adaptive Output Feedback Control of Uncertain Multi-Input Multi-Output Systems using Single Hidden Layer Networks," *International Journal of Control*, 2002.

[12]Johnson, E., and Calise, A.J., "Feedback Linearization with Neural Network Augmentation applied to X-33 Attitude Control," *AIAA-2000-4157 Guidance, Navigation and Control Conference*, Denver, CO, August 2000.

[13]Johnson, E., and Calise, A.J., "Neural Network Adaptive Control of Systems with Input Saturation," *Proc of the American Control Conference*, Arlington, VA, June 2001, pp. 3527-3532.

[14]Isidori, A., *Nonlinear Control Systems,* Springer, 1995.

[15]Calise, A.J., Hovakimyan, N., and Idan, M., "Adaptive Output Feedback Control of Nonlinear Systems using Neural Networks," *Automatica*, Vol. 37, No. 8, August 2001.

[16]Hovakimyan, N., Lee, H., and Calise, A.J., "On approximate NN realization of an unknown dynamic system from its input-output history," *Proc of the American Control Conference*, Chicago, IL, June 2000, pp. 919-923.

[17]Lavretsky, E., Hovakimyan, N., and Calise, A.J, "Upper Bounds for Approximation of Continuous-Time Dynamics Using Delayed Outputs and Feedforward Neural Networks," *IEEE Transactions on Automatic Control*, Vol. 8, Sept. 2003, pp.1606-1610.

[18]Idan, M., Johnson, M., and Calise, A.J., "A Hierarchical Approach to Adaptive Control for Improved Flight Safety," *AIAA-2001-4209 Guidance, Navigation and Control Conference*, Montreal, Canada, August 2001.